Submitted to the 30th International Conference on High-Energy Physics ICHEP2000,
Osaka, Japan, July 2000

Measurement of Dijet Cross-Sections with Leading Neutrons in Photoproduction at HERA

H1 Collaboration

Abstract

An analysis is presented of dijets in photoproduction where a leading neutron with an energy $E_n > 400$ GeV and angle $\theta_n < 0.8$ mrad with respect to the proton direction is detected. The average photon-proton center-of-mass energy is about $< W_{\gamma p} >\approx 200$ GeV. Differential cross sections $\mathrm{d}\sigma/\mathrm{d}E_T^{jet}$ and $\mathrm{d}\sigma/\mathrm{d}\eta^{jet}$ are measured where E_T^{jet} and η^{jet} are jet transverse energy and pseudorapidity. Furthermore differential cross–sections in x_γ^{jet} and x_π^{jet} are given where x_γ^{jet} is the fraction of the photon momenta entering the hard scattering, and x_π^{jet} is the fraction of pion momenta in a model where the interaction proceeds via exchange of a pion. The Monte Carlo predictions based on standard photoproduction processes or based on the one-pion-exchange model and using different parametrizations for the pion structure function are compared to the measurements.

Abstract: 959
Parallel session: PA-02
Plenary talk: PL-12

1 Introduction

The cloud of virtual pions contained in the proton plays an important dynamical role in the structure of the nucleon. It has been shown (e.g. in [1, 2, 3]) that the pion-pole contribution to Deep Inelastic Scattering (DIS) can reliably be determined by studying the production of highly energetic forward neutrons. The parton distributions of the pion in the region of $x \gtrsim 0.2$ have been constrained by fixed target experiments. Additionally, the analysis of leading neutron data in DIS at HERA performed by the H1 Collaboration [4] made possible for the first time a measurement os the pion structure function at small Bjorken-x ($\sim 10^{-3} - 10^{-2}$).

Another sensitive probe of the structure of interacting particles is the production of high p_T jets in hard hadronic interactions. Thus, by tagging dijet events with a leading neutron in the final state, it should be possible to extract information on the parton distributions in the pion. In this paper we present measurements of the jet production differential cross-sections in photoproduction for events with a leading neutron in the final state which has energy $E_n > 400$ GeV and angle $\theta_n < 0.8$ mrad. The cross-sections are measured differentially in jet transverse energy E_T^{jet}, in pseudorapidity η^{jet}, and in the momentum fractions of the photon and the pion carried by the interacting partons, x_γ^{jet} and x_π^{jet}. Different predictions in the form of Monte Carlo simulations are compared to the measurements.

2 Event selection

In this analysis data are used which were collected by the H1 detector in the years 1996–97 corresponding to an integrated luminosity of $19.2\ \mathrm{pb}^{-1}$. Photoproduction events are selected by measuring the scattered electron in the electron detector of the luminosity system. The scaled photon energy $y \equiv E_e/E_e^0$ is required to be within $0.3 < y < 0.65$, where E_e is the energy of the scattered electron in the electron detector and E_e^0 is the electron beam energy (27.5 GeV). These requirements restrict the photon virtuality to be $Q^2 < 0.01\ \mathrm{GeV}^2$ and the total center-of-mass energy of the photon–proton system to be $156 < W_{\gamma p} < 242$ GeV. Furthermore, the z-coordinate of the reconstructed vertex is required to lie within 30 cm of the nominal interaction point. Jets are identified in the Liquid Argon Calorimeter (LAr) by means of a cone-type algorithm with a cone size of $R = \sqrt{\Delta\eta^2 + \Delta\phi^2} = 1$. Finally, events are selected which have exactly two jets with transverse energy $E_T^{jet} > 4$ GeV and pseudorapidity $-1 < \eta^{jet} < 2$.

Leading neutrons are detected in the Forward Neutron Calorimeter (FNC) which consists of lead and scintillator fibres and which is located 107 m away from the nominal H1 interaction point in the proton beam direction. (for details see [4]). The acceptance of the FNC is defined by the aperture of the HERA beam pipe magnets and it corresponds to neutron scattering angles of about $\theta_n \lesssim 0.8$ mrad. For this analysis the energy of the neutron in the FNC is required to be $E_n > 400$ GeV.

In total, about 320,000 dijet events are selected, from which 3187 events satisfy $E_n > 400$ GeV. If the cut on jet transverse energy is increased from 4 to 7 GeV, then the total dijet data sample is reduced to about 41,000 events and the neutron sample to 327 events.

3 Monte Carlo models

To correct the data distributions for biases and losses due to the apparatus and to compare the theoretical models with data, the POMPYT 2.6 [5] and PYTHIA 5.7 [6] Monte Carlo programs are used.

POMPYT simulates leading neutron production using pion exchange. In this program, the cross-section for leading neutron production is proportional to the product of a pion flux factor and a pion structure function. In the present analysis the pion flux factor is taken from Holtmann et al. [1]. The pion parton distributions are simulated according to the GRV-π-LO parameterizations [7]. For the comparisons with data, additional POMPYT predictions based on different parton distributions are also used [8].

PYTHIA simulates leading neutron production using the JETSET string fragmentation model. The program includes the possibility for additional hard interactions between the remnant partons. These *multiple interactions* increase the underlying energy in the event and improve the description of jets and energy flow in inclusive hard photoproduction measurements [9]. When comparing PYTHIA predictions with data, simulations are used both with and without multiple interactions.

The parton densities in the proton are generated in PYTHIA according to the GRV-LO parameterization [10]. Both PYTHIA and POMPYT use the GRV-LO parameterizations for the parton densities in the photon [11].

4 Results

Figure 1 shows the distributions of the energy of the neutrons measured in the FNC uncorrected for inefficiency and acceptance. Also shown are the expectations from the POMPYT and PYTHIA Monte Carlo simulations (with and without multiple interactions). The standard JETSET fragmentation model (used by PYTHIA) fails to reproduce acceptably the neutron energy spectrum, predicting a distribution which is shifted towards lower energies. POMPYT, on the other hand, describes the energy spectrum well for $E_n \gtrsim 400$ GeV, thereby demonstrating the necessity in the FNC energy spectrum for a colour singlet component in the proton manifest in the form of pion exchange and its explicit contribution to leading neutron production. The large difference between data and Monte Carlo at low E_n is due to background from neutral electromagnetic particles (π^0, γ-s) which are present in the data but not in the Monte Carlo simulations used for this analysis. For neutron energies above $E_n > 400$ GeV this contribution is below 1% and is neglected in the following. The high-energy tail of the neutron energy spectrum is due to the small attenuation length of scintillating fibres (1.7 ± 0.2 m) in the FNC which leads to an over-estimation of the incident particle's energy and worsening of energy resolution ($\sigma(E)/E \approx 20\%$ for energies between 300 and 800 GeV) [4].

To calculate the cross-sections, the data have been corrected for trigger efficiency, the neutron detection efficiency of the FNC ($93\% \pm 5\%$)[4] and the acceptances of the FNC and electron detector. The corrections for detector effects were calculated using the POMPYT Monte Carlo simulation which in general describes well all measured distributions.

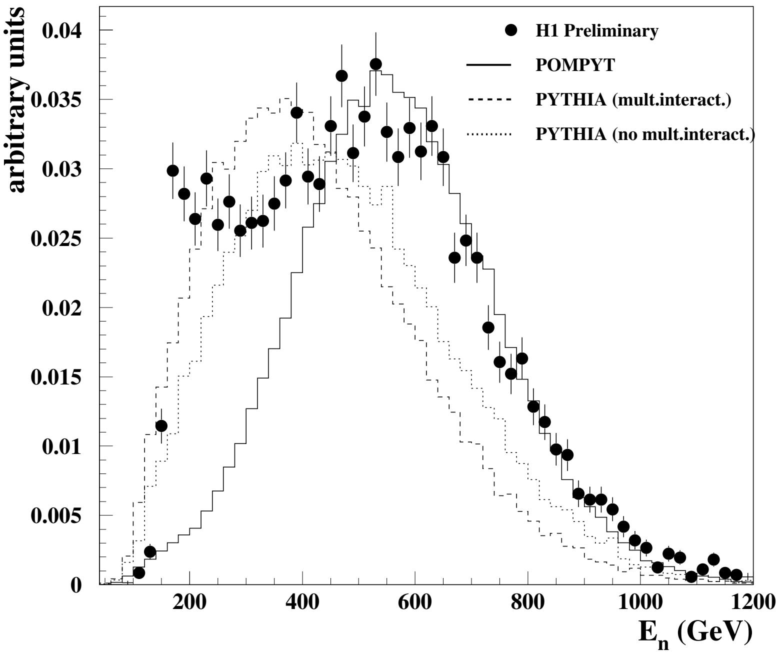

Figure 1: The distributions of leading neutron energy E_n for data and POMPYT and PYTHIA Monte Carlo.

The resulting cross-sections for jet production with $E_T^{jet} > 4$ GeV and events with $E_n > 400$ GeV and $\theta_n < 0.8$ mrad are shown in Figs.2–3. E_T^{jet} and η^{jet} are the jet transverse energy and pseudorapidity (positive η^{jet} corresponds to the proton direction). x_γ^{jet} and x_π^{jet} are the fractional momenta of the photon and pion carried by the partons involved in hard interaction. x_γ^{jet} and x_π^{jet} are calculated from the jet E_T^{jet} and η^{jet} as follows:

$$x_\gamma^{jet} = (E_{T,1}^{jet} e^{-\eta_1^{jet}} + E_{T,2}^{jet} e^{-\eta_2^{jet}})/2yE_e^0 \qquad x_\pi^{jet} = (E_{T,1}^{jet} e^{\eta_1^{jet}} + E_{T,2}^{jet} e^{\eta_2^{jet}})/2(E_p^0 - E_n)$$

Here $E_e^0 = 27.5$ GeV and $E_p^0 = 820$ GeV are the incident electron and proton beam energies. In the figures the inner error bars represent the statistical errors, while the outer error bars show the quadratic sum of statistical and systematic errors combined. The total systematic errors are about 27%.

In Figure 2 the POMPYT and PYTHIA predictions are compared with the measured cross-sections. Both the PYTHIA simulation without multiple interactions and the POMPYT simulation predict somewhat higher cross–sections than measured, and they do not describe the dependence on pseudorapidity in that they predict higher cross-section at low pseudorapidities. When multiple interactions are included in the PYTHIA model the predicted cross-section is higher than the measurements by a factor 3.

In the framework of the one-pion-exchange model in POMPYT, the sensitivity of the measurement to different choices for the pion structure function [8] is presented in Figure 3. It is clear that the remedy for the disagreement between the POMPYT prediction and the measurements is not to be found in a different choice of otherwise acceptable parametrisations of the pion structure function.

Figure 4 shows similar cross-sections but after increasing the cut on the jet transverse energy from 4 to 7 GeV. At higher jet energies all Monte Carlo models used for comparison describe the data distributions well, both in shape and normalization. We note that with this higher E_T^{jet} cut there is a larger fraction of direct photoproduction ($x_\gamma \approx 1$) as expected kinematically.

Figure 5 shows the sensitivity of the POMPYT prediction of the cross sections to the same choices as above for the pion structure function. It is clear that the present level of systematic uncertainty in the measurement means that no preference for any of the pion structure function parameterizations can yet be given.

5 Summary

Measurement of the differential jet cross-sections are presented as function of E_T^{jet}, η^{jet}, x_γ^{jet} and x_π^{jet} in photoproduction (in the kinematic range $Q^2 < 0.01$ GeV^2, $0.3 < y < 0.65$) for events with an energetic forward neutron (leading neutron) in the final state.

A model which does not include pion exchange fails to describe the neutron energy spectrum. A model which includes one pion exchange describes the neutron energy spectrum well, thereby establishing the need for a colour singlet component of proton structure which is manifest in the form of pion exchange and leading neutron production. The model also reproduces the observed jet differential production cross sections for $E_T^{jet} > 7$ GeV, but fails for lower $E_T^{jet} > 4$ GeV. Within the present experimental uncertainties of this measurement, it is not yet possible to discriminate between different parameterizations of the pion structure function.

References

[1] H. Holtmann et al., *Phys.Lett.* **B338** (1994) 363.

[2] B. Kopeliovich, B. Povh and I. Potashnikova, *Z. Phys.* **C73** (1996) 125.

[3] M. Przybycień, A. Szczurek and G. Ingelman, *Z. Phys.* **C74** (1997) 509.

[4] H1 Collaboration, *Eur. Phys.J.* **C6** (1999) 587.

[5] P.Bruni, G. Ingelman, *Proceedings of the Europhysics Conference, Marseille, France, July 1993, p.595*;
see also http://www3.tsl.uu.se/thep/pompyt

[6] PYTHIA Version 5.722, T. Sjöstrand, *Comp. Phys. Comm.* **82** (1994) 74;
T. Sjöstrand, “PYTHIA 5.7 and JETSET 7.4”, CERN-TH.7112/93 (1993) (revised Feb. 1994).

[7] M. Glück, E. Reya and A. Vogt, *Z. Phys.* **C53** (1992) 651.

[8] J.F. Owens, *Phys.Rev.* **D30** (1984) 943;
P.J. Sutton et al., *Phys.Rev.* **D45** (1992) 2349.

[9] H1 Collaboration, *Z. Phys.* **C70** (1996) 17.

[10] M. Glück, E. Reya and A. Vogt, *Z. Phys.* **C53** (1992) 127.

[11] M. Glück, E. Reya and A. Vogt, *Phys. Rev.* **D46** (1992) 1973.

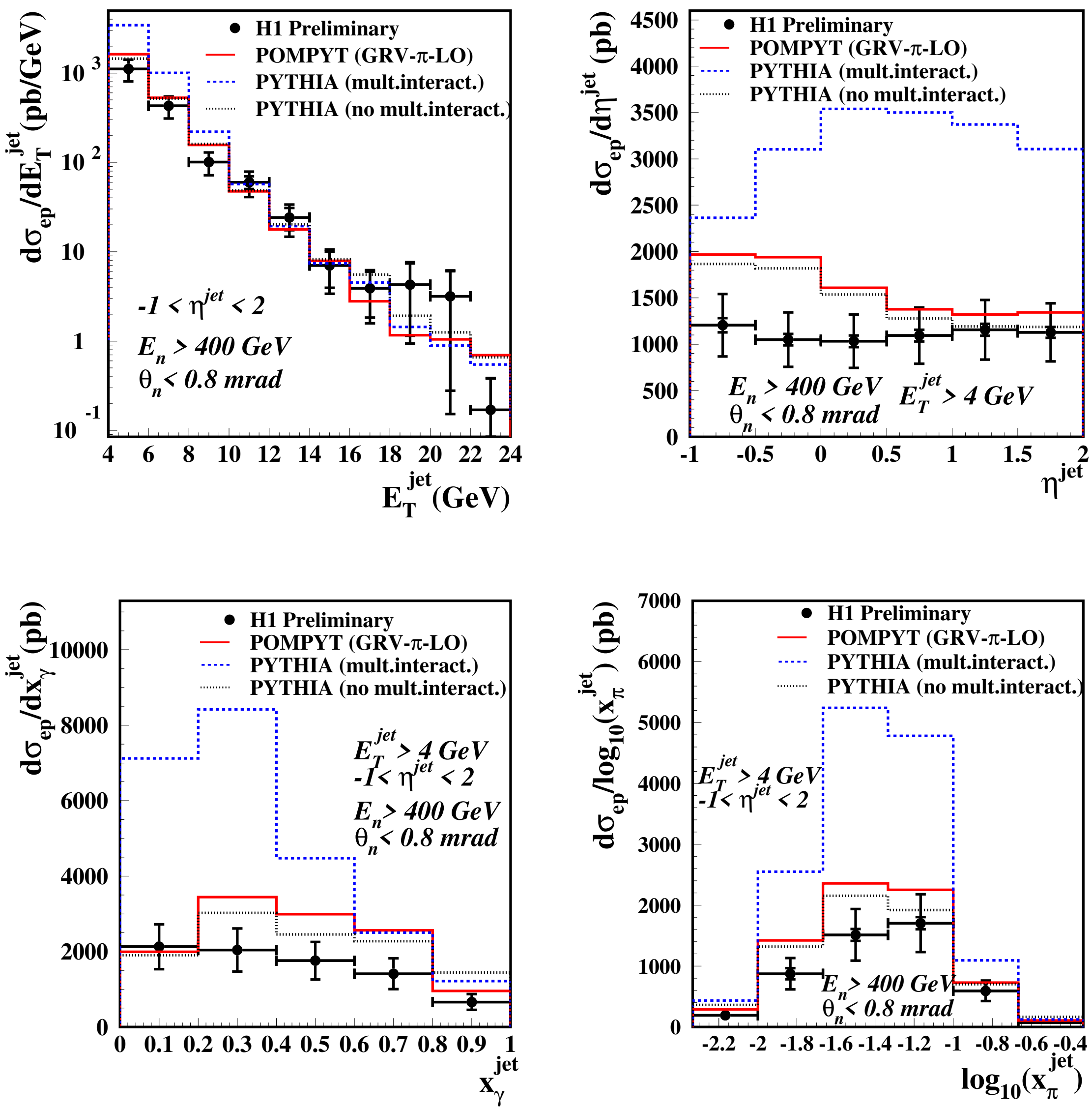

Figure 2: Dijet differential cross-sections as function of jet E_T^{jet}, η^{jet}, x_γ^{jet} and x_π^{jet} for events with $E_T^{jet} > 4$ GeV, $-1 < \eta^{jet} < 2$ and with leading neutrons $E_n > 400$ GeV, $\theta_n < 0.8$ mrad. Cross-sections correspond to kinematic range $Q^2 < 0.01$ GeV^2 and $0.3 < y < 0.65$. The POMPYT and PYTHIA Monte Carlo predictions are compared to the measurements.

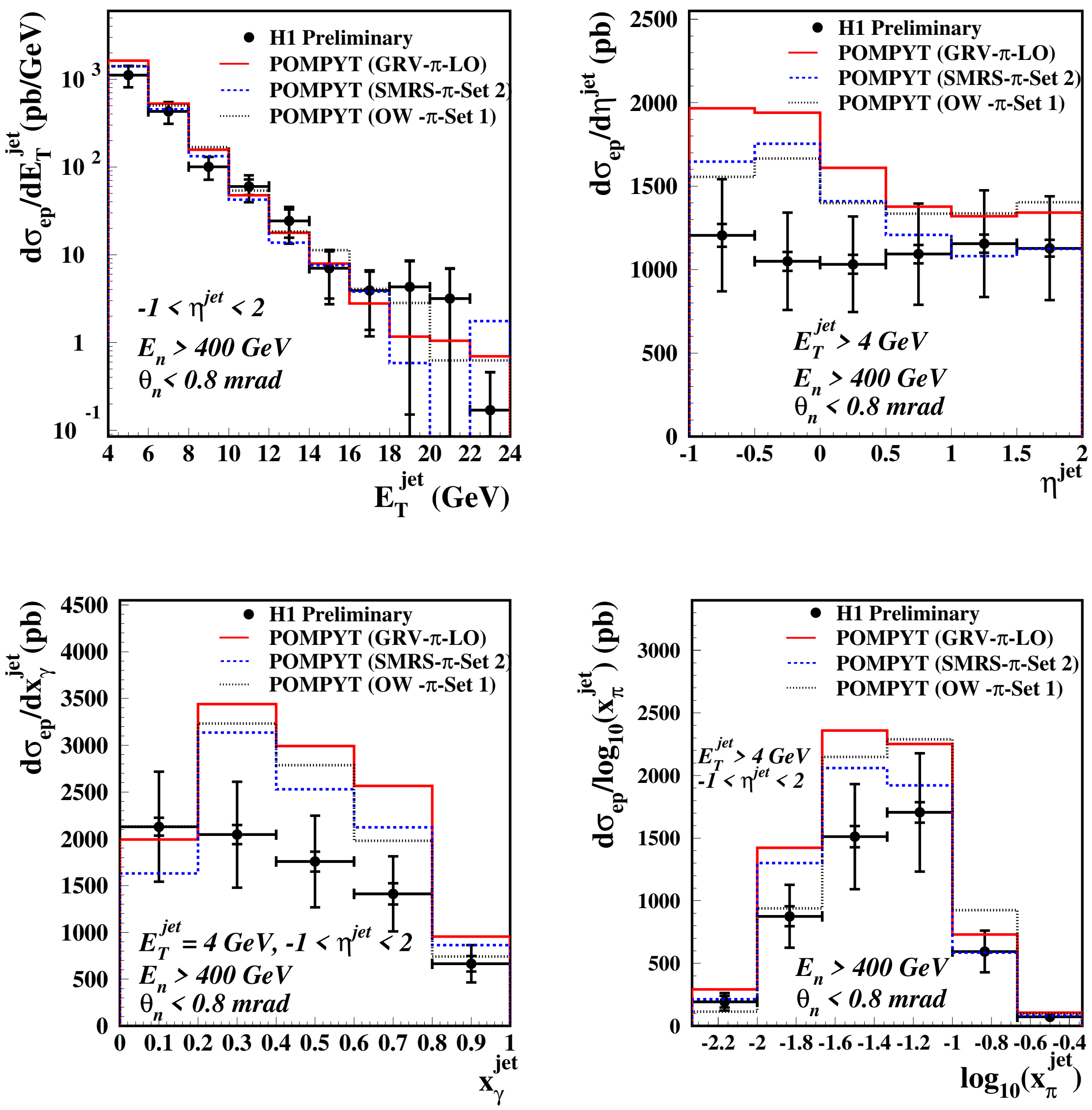

Figure 3: Dijet differential cross-sections as function of jet E_T^{jet}, η^{jet}, x_γ^{jet} and x_π^{jet} for events with $E_T^{jet} > 4$ GeV, $-1 < \eta^{jet} < 2$ and with leading neutrons $E_n > 400$ GeV, $\theta_n < 0.8$ mrad. Cross-sections correspond to kinematic range $Q^2 < 0.01$ GeV^2 and $0.3 < y < 0.65$. The POMPYT Monte Carlo predictions using different parameterizations for the parton distributions in the pion are compared to the measurements.

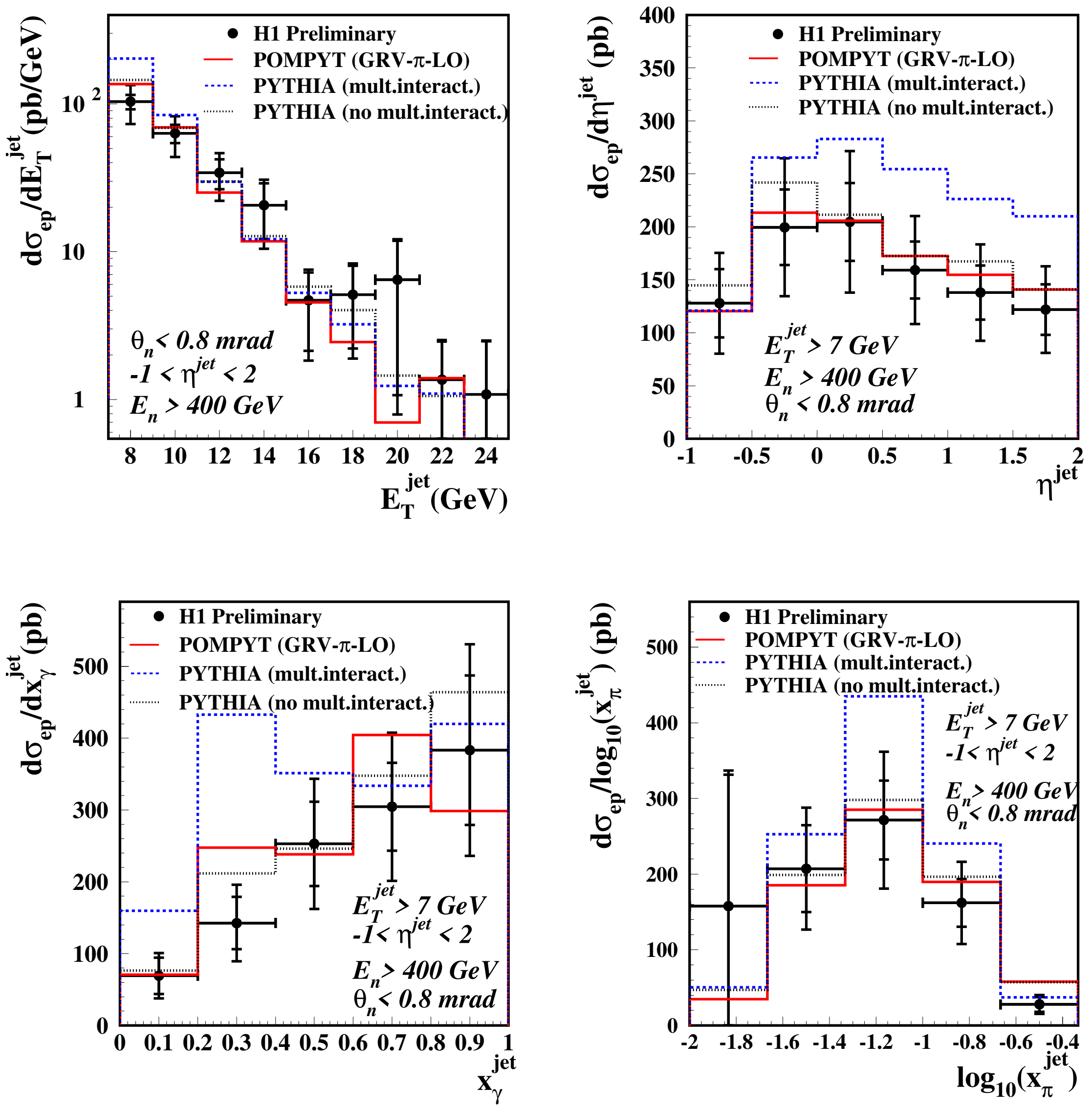

Figure 4: Dijet differential cross-sections as function of jet E_T^{jet}, η^{jet}, x_γ^{jet} and x_π^{jet} for events with $E_T^{jet} > 7$ GeV, $-1 < \eta^{jet} < 2$ and with leading neutrons $E_n > 400$ GeV, $\theta_n < 0.8$ mrad. Cross-sections correspond to kinematic range $Q^2 < 0.01$ GeV^2 and $0.3 < y < 0.65$. The POMPYT and PYTHIA Monte Carlo predictions are compared to the measurements.

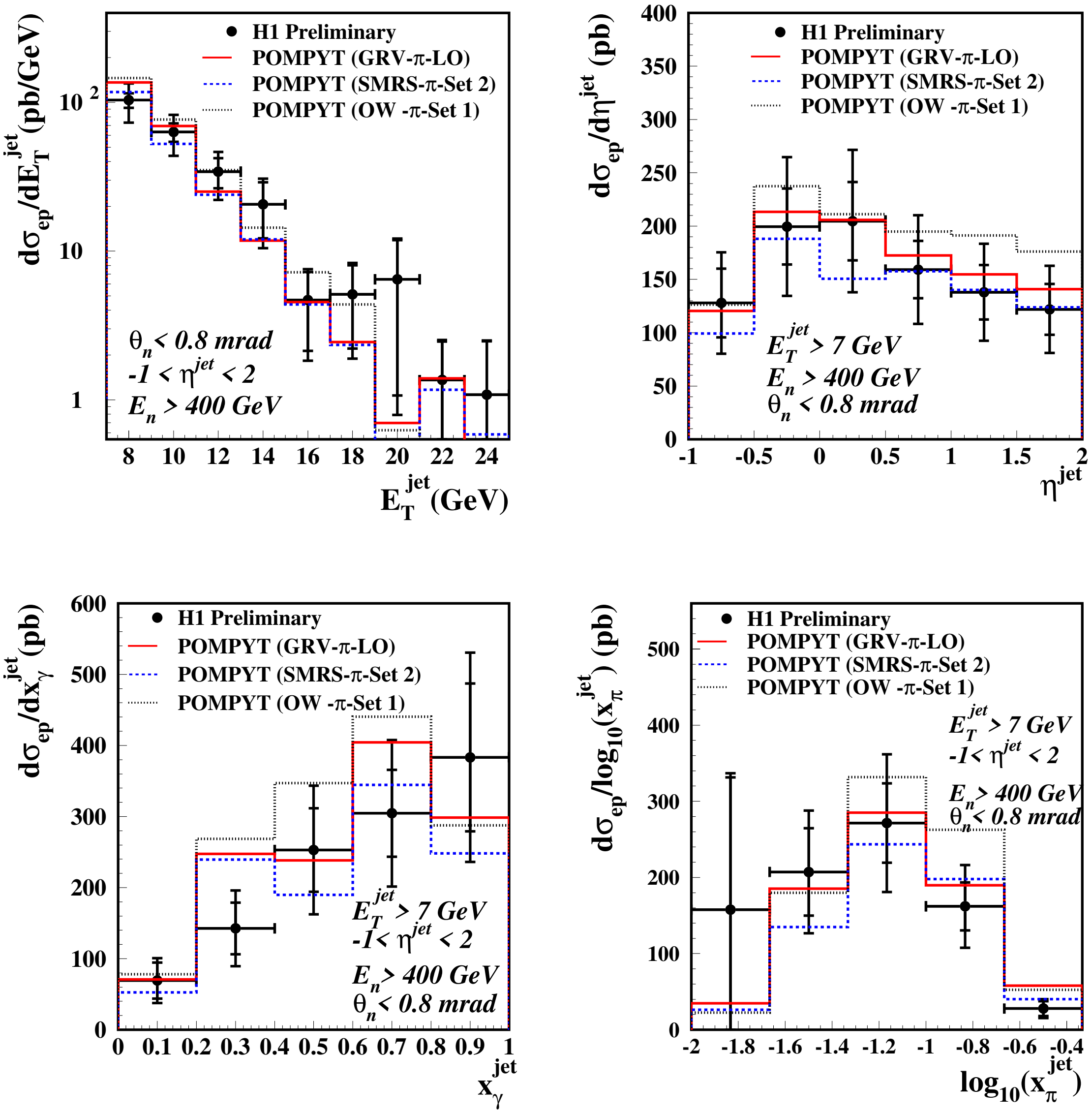

Figure 5: Dijet differential cross-sections as function of jet E_T^{jet}, η^{jet}, x_γ^{jet} and x_π^{jet} for events with $E_T^{jet} > 7$ GeV, $-1 < \eta^{jet} < 2$ and with leading neutrons $E_n > 400$ GeV, $\theta_n < 0.8$ mrad. Cross-sections correspond to kinematic range $Q^2 < 0.01\ \mathrm{GeV}^2$ and $0.3 < y < 0.65$. The POMPYT Monte Carlo predictions using different parameterizations for the parton distributions in the pion are compared to the measurements.